A post-disaster assessment on a storm-induced flood and associated coastal dispersal of the river-derived suspended radiocesium originated from the Fukushima nuclear accident

Yusuke Uchiyama[1*], Natsuki Tokunaga[1#]

[1]*Department of Civil Engineering, Kobe University, Japan*
Email: uchiyama@harbor.kobe-u.ac.jp
*corresponding author, # presenter

Abstract

Niida River, Fukushima, Japan, is well known to be a source of highly contaminated suspended radiocesium to the ocean, which is originated from the Fukushima Dai-ichi Nuclear Power Plant during the accidental leakage occurred in March 2011. We examined the oceanic dispersal and inventories of the sediments and suspended radiocesium in the ocean floor derived from Niida River, using a quadruple nested JCOPE2-ROMS 3D circulation model in a very high resolution configuration, coupled with a 3D multi-class sediment transport model, the iRIC-Nays 2DH river sediment model, the SWAN spectral wave model, and a static radiocesium absorption model. A particular attention was paid to the storm and subsequent flood event associated with Typhoon 201326 (Wipha) passed off the Fukushima Coast in October 2013, which provoked an enormous amount of precipitation, and subsequent riverine freshwater discharge and sediment fluxes to the ocean. With a guide of several *in situ* observed data, we carried out a quantitative assessment of the accumulation and erosion of the sediments and resultant suspended radiocesium distribution around the river mouth and nearshore areas along the Fukushima Coast.

Keywords: nuclear accident, river-derived suspended radiocesium, inventory analysis, ROMS

Introduction

A nuclear accident occurred at the Fukushima Dai-ichi Nuclear Power Plant (hereinafter FNPP) in March 2011 due to catastrophic tsunamis associated with the Great East Japan Earthquake. Since then, researches have been carried out with limited measurement during the initial stage of the post-accident aided by numerical models to evaluate that the ocean has received 3-10 PBq as the direct release of radiocesium 137 (^{137}Cs) from the FNPP (e.g., Tsumune et al., 2012 [1], 2013 [2]; Kamidaira et al., 2018 [3]). However, the coastal dispersal of the radionuclides is affected not only by the direct release but also by atmospheric fallout and discharge from the rivers. The last process introduces a time lag behind the direct release with hydrological process because the radionuclides mostly attach to suspended particles, i.e., sediments, which are transported quite differently to the dissolved matter in the water (e.g., Misumi et al., 2014 [4]). Those suspended radionuclides have been discharged from the river mouths intermittently with infrequent flood events. They recirculate in the ocean as they readily sink to the ocean bottom due to settling, counteracted by resuspension back in the water by abrupt increase of bed shear stresses. Therefore, suspended radionuclides are anticipated to remain largely near the river mouths and coastal areas because of less mobility, leading to continuous addition of radioactivity to ambient water and marine flora and fauna.

Niida River is a second level (i.e., maintained not by the central but by a local government) river flowing through Fukushima Prefecture with the mouth located at ~24 km north of the FNPP. It has a watershed characterized by quite high terrestrial radioactivity due to the initial atmospheric fallout upon the accident. Hydrological processes have led to weathering of terrestrial surface sediments that are subsequently gathered in the river channel to be transported downstream particularly during flood events. Hence, Niida River has been recognized as a source of highly contaminated suspended radionuclides to the ocean up until the present. To understand such processes, and to quantify possible influences of the river-derived suspended radionuclides and their inventory in the ocean off Fukushima, we conducted a two-month numerical hindcast including the storm and flood event associated with Typhoon 201326 (Wipha) passed off the Fukushima Coast in October 2013 using a coupled river-ocean-wave-sediment model along with a static absorption model to account for radiocesium attached to sediments.

The Coupled Downscaling Model

A comprehensive, inter-disciplinary approach is essential to deal with such complicated process of the radionuclide in the nature that requires considering atmospheric, hydrological, limnological and oceanic processes. To this end, we developed a coupled numerical model that investigates the behavior of land-derived sediments and suspended radionuclides in the marine environment near the river mouths. First, to account for large-scale oceanic variability responsible for the 3D flow field near the Niida river mount, we configured a downscaling ocean model based on the Regional Oceanic Modeling
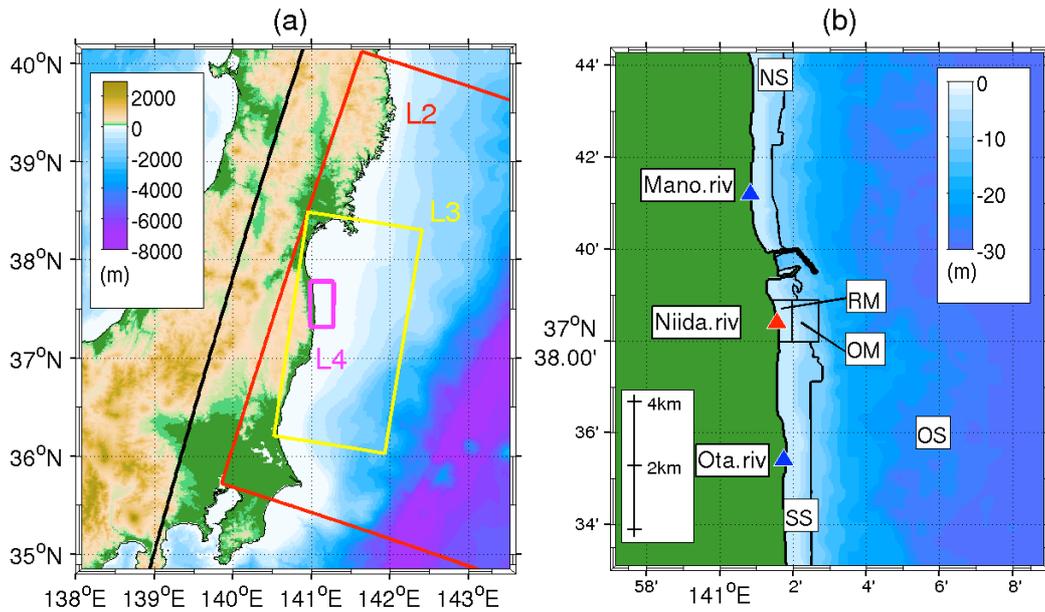
Figure 1: (a) A hierarchy of the quadruple nested JCOPE2-ROMS downscaling model domain around the Fukushima coast. The colored rectangle frames account for ROMS-L1 (black, at lateral resolution of 3 km), L2 (red, 1 km), L3 (yellow, 250 m), and L4 (magenta, 50 m). (b) An enlarged area near the mouth of Niida River shown by the red triangle. Mouths of the tow neighboring rivers (Mano and Ota rivers) are also presented by blue triangles. Black lines correspond to the perimeter of segments used in the flux budget analysis. Background colors indicate depth in m.

Table 1: Numerical configuration of the Niida River model (ROMS-L4)

Computational period	October 1, 2013–November 30, 2013
Grid cell numbers	1,024 × 512 × 32 vertical s-layers, lateral grid resolution: 50 m
Lateral B.Cs.	ROMS-L3 (2-hourly average)
Surface wind stress	Japan Meteorology Agency GPV-MSM (hourly)
Other surface fluxes	NOAA COADS (monthly climatology)
Sea surface temperature (SST)	AVHRR Pathfinder (monthly averaged): for heat flux correction
River discharge	Niida River: iRIC-Nays 2DH model hindcast (hourly average) The other rivers: HYDREEMS hindcast (daily average)
Bathymetry	Central Disaster Prevention Council, the Cabinet Office of Japan (10 m)
Wind wave and swell	Downscaling CWM-SWAN model hindcast (3-hourly average)

System, ROMS (Shchepetkin and McWilliams, 2005 [5]), in a quadruple nested configuration by 1-way offline nesting approach (**Figure 1**). Daily-mean velocity and density fields of the JCOPE2 oceanic reanalysis (Miyazawa et al., 2009 [6]) were utilized as the lateral boundary condition and the initial condition of the outermost ROMS-L1 model at a grid resolution of 3 km. We successively downscaled it to ROMS-L4 model with a horizontal resolution of 50 m by following the well-established methodology described in Mason et al. (2011) [7], Uchiyama et al. (2017a [8]; 2017b [9]), and Tada et al. (2018) [10]. The GPV-MSM operational weather product of the Japan Meteorological Agency (JMA) primarily provided the atmospheric forcing to the ROMS models. We introduced the Eulerian passive tracer module (e.g., Uchiyama et al., 2014 [11]; Uchiyama et al., 2018 [12]) for dispersal of dissolved radioactive ^{137}Cs released from the point source where the FNPP is located by using a leakage submodel proposed in Tsumune et al. (2012) [1]. The numerical configurations for the ROMS-L4 model are listed in **Table 1**.

Second, we developed a multi-class non-cohesive suspended sediment transport model with a two-layered stratigraphy model based on Blaas et al. (2007) [13]. In the present study, we consider three classes of sediments, namely fine sand, silt and clay fractions. The corresponding settling velocity and other model variables are summarized in **Table 2**. Sediments are suspended when the bed skin stress exceeds the prescribed critical stress. The bed skin stress is evaluated from a combined wave-current bed shear stress model of Soulsby (1995) [14] as a function of an empirical combination the log-layer current stress and a wave-induced bottom stress. The two-layer stratigraphy model consists of an active layer of 3 mm thick sitting on the top of a substrate of 10 m. The active layer is defined as the thin interface between water column and sediment bed. When the bed erodes, the sediments in the substrate is mixed with the active layer to compensate for the sediment loss. On the other hand, when sediments deposit, the bottom portion of the active layer is merged with the substrate to keep 3 mm thickness of the active layer. This regional 3D sediment transport model was activated in the innermost ROMS-

Table 2: Model parameters for the multi-class sediment transport model

class	d μm	ρ_s kgm^{-3}	w_s mms^{-1}	E_u Kgm^{-2}s^{-1}	τ_{cr} Nm^{-2}
sand	125	2650	9.4	2.5×10^{-3}	0.15
silt	24	2650	0.4	1.0×10^{-4}	0.07
clay	4	2650	0.1	1.0×10^{-4}	0.02

where d: median grain size, r_s: sediment dry density, w_s: settling velocity, E_u: resuspension rate, τ_{cr}: critical bed shear stress for resuspension, $\lambda = 0.4$: porosity (constant), $d_a = 3$ mm: thickness of the active layer (initial thickness of the substratum: 10 m).
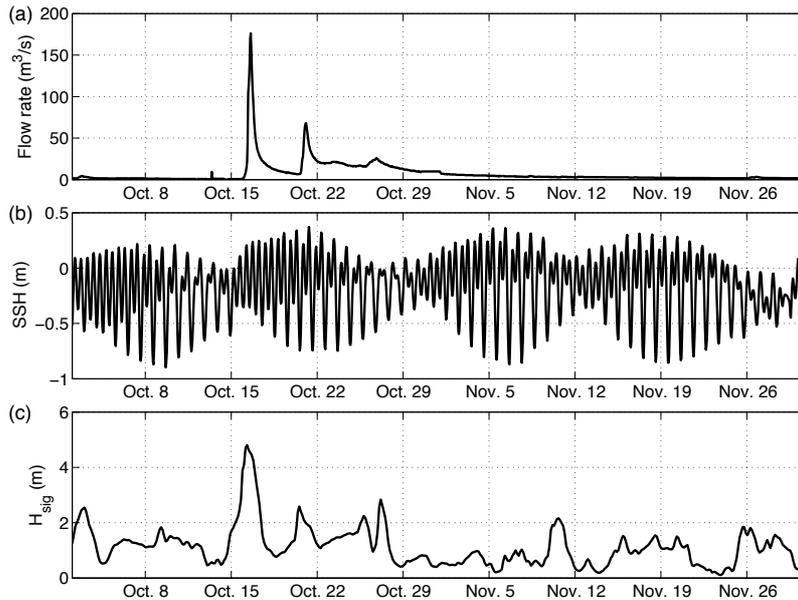

Figure 2: Time series of (a) hourly discharge from the Niida river mouth evaluated by the iRIC-Nays 2DH model, (b) free-surface elevation at 1 km off the Niida river mouth computed by the ROMS-L4 model, and (c) significant wave height computed by the CWM-SWAN model at the same location as that of (b). The displayed are for the entire two-month analysis period from October 1–November 30, 2013. Notice Typhoon Wipha approached on October 16.

L4 model. Third, to properly account for spatiotemporally varying wave effects on the bed shear stress at the ocean floor in the sediment model, a third generation spectral wave model SWAN (Booij et al., 1999 [15]) at a horizontal resolution of 1 km was used in the present study, nested in the JMA GPV-CWM wave reanalysis product at 5–6 km resolution. A static absorption submodel of ^{137}Cs to sediment particles were employed to evaluate behavior of suspended ^{137}Cs in the ocean.

Finally, the river discharges to the ocean were basically obtained as daily-averaged volume fluxes at each river mouth using a surface run-off model HYDREEM. A regional HYDREEM hindcast was conducted at Central Research Institute of Electric Power Industry, CRIEPI (courtesy of Dr. D. Tsumune), driven by measured precipitation field for the entire Tohoku/Fukushima region. On the contrary, for Niida River, we exploited a more sophisticated iRIC-Nays2DH model, which accounts for depth-integrated shallow-water river flow and associated multi-class sediment transport (http://i-ric.org/en/software/?c=17). The iRIC-Nays2DH hindcast was performed at the Civil Engineering Research Institute for Cold Region and at Hokkaido University (courtesy of Dr. T. Iwasaki and Prof. Y. Shimizu). It provided hourly discharge and three-class sediment concentrations (viz., fine sand, silt, and clay) at the Niida river mouth. These river model hindcasts introduced freshwater inputs from all the river mouths located in the L4 domain and multi-class sediment fluxes at the Niida river mouth. The developed river-ocean-wave-sediment coupled model was utilized to carry out a two-month hindcast including the storm and flood event associated with Typhoon 201326 (Wipha) passed off the Fukushima Coast in October 2013.

Results and Discussions

Figure 2 displays time series plots of the Niida river discharge, sea surface height (SSH) and significant wave height
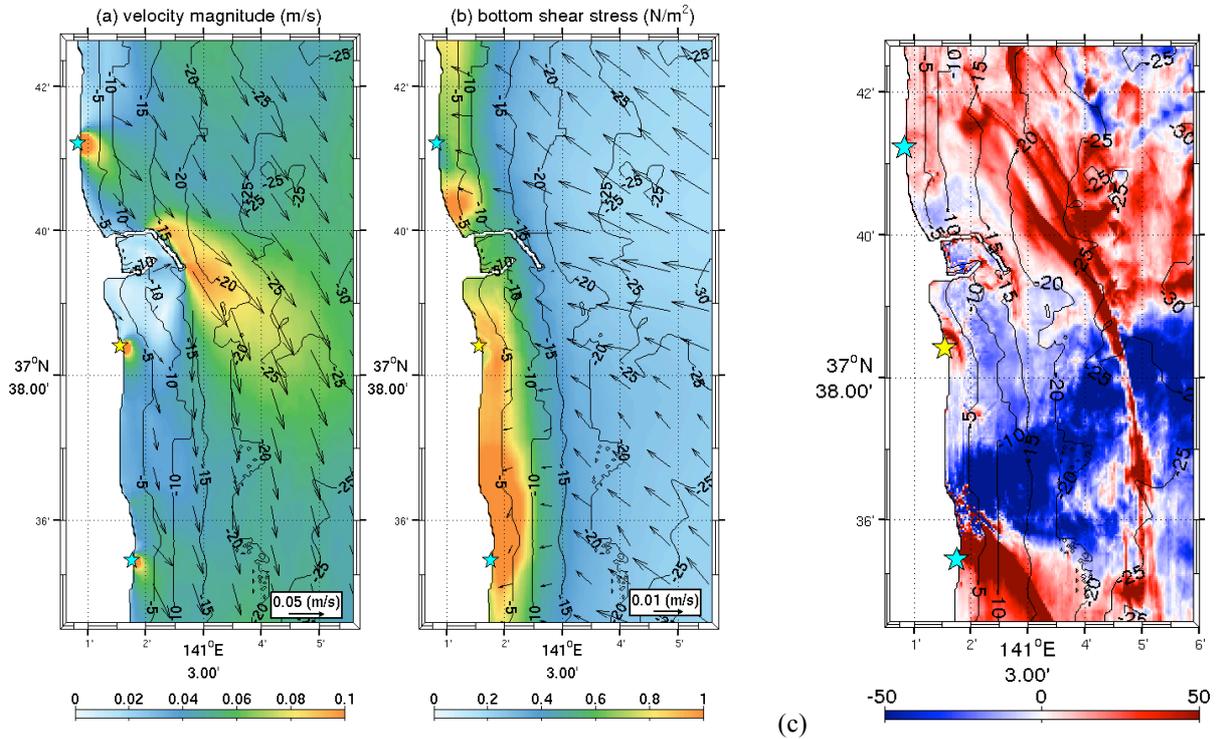
Figure 3: Time-averaged (a) surface velocity vectors (subsampled) and their magnitude in color, and (b) near-bed velocity vectors and bes shear stresses in color. The averages were taken for the whole model period (Oct. 1–Nov. 30). Star marks are river mouths; yellow star is the Niida river mouth; and black contours are isobaths in m. (c) Cumulative deposition (accretion, redish) and resuspension (erosion, bluish) integrated since Oct. 1 until Nov. 30, 2013 (unit: kgm^{-2}) as a sum of the three size classes.

near the mouth. On Oct. 16 when the typhoon came closest to the Niida river mouth area, the river discharge increased as large as 180 m^3/s due to heavy precipitation associated with the storm (**Figure 2a**), during about four spring-neap tidal cycles (**Figure 2b**). The typhoon provoked a quite stormy condition with maximum wind speed at 20 m/s and significant wave height of 4.6 m (**Figure 2c**). The river discharge was increased twice again after the typhoon passage, while the second and third peaks show only ~60 and 40 m^3/s.

Temporally averaged surface currents were approximately in the alongshore direction toward SSE (**Figure 3a**). The current speed was markedly enhanced near the river mouths, coastline bends, and the harbor structures (breakwaters) located north of the Niida river mouth. By contrast, time averaged near-bed currents indicate prevailing shoreward currents that compensate for the surface currents, leading to coastal upwelling (**Figure 3b**). The associated bed shear stress (color) exhibits quasi-periodicity in the alongshore direction in the nearshore shallow area with the depths less than ~10 m. Overall, the nearshore bed shear stress exceeded 0.5 N/m^2 due mainly to waves, which corresponds to the resuspension dominant condition for all the three sediment size classes.

Resultant cumulative resuspension and deposition are represented by bed accretion and erosion due to combined influences from all the three sediment size classes (**Figure 3c**). Accretion (redish colors) is prevailed in a narrow area right in front of the Niida river mouth, while erosion (bluish colors) dominates extensively in the offshore of the mouth. Near-surface seaward currents developed near the mouth (**Figure 3**) serves as a node for sedimentation in the shallow area; erosive (accretive) areas are formed in the north (south) of the mouth. Topographies near the river mouths and harbor structures entrain alongshore sediment transport effectively, resulting in alternative appearance of erosive and accretive patterns in the alongshore direction. Gravitational circulations associated with buoyant riverine freshwater input into the ocean induce shoreward near-bed currents (**Figure 3b**) and thus promote the shoreward sediment transport. As a result, sedimentation predominantly occurred near the river mouths.

Figure 4 shows temporal evolution of suspended ^{137}Cs in the marine bed sediments derived from Niida River. Instantaneous radioactivity contained in all the three sediment size classes in unit bed area (Bq/m^2) is depicted for Oct. 14 (before Wipha), Oct. 16 (Wipha was closet to Niida River), Oct. 18 (two days after Wipha showing influences of heavy precipitation and the associated flood), Oct 31 (two weeks after Wipha), and Nov. 30 (six week after Wipha) at 0:00 UTC on each day. The radioactivity is computed for all the three sediment size classes. Before the Wipha-driven flood (Oct. 14 and 16), suspended ^{137}Cs was confined near the shore and distributed largely on the south of the mouth due to southward sediment transport. After Wipha passed off the Fukushima on Oct. 18, the subsequent heavy rainfall and associated flood induced a pronounced ^{137}Cs accumulation in the vicinity of the mouth within a radius of ~2 km, followed by gradual southward transport and then dispersed and diluted extensively (Oct. 31 and Nov. 30). Furthermore, the harbor structure (of a power plant facility) at the north of Niida river mouth significantly collected sediments to induce accretion with the harbor.
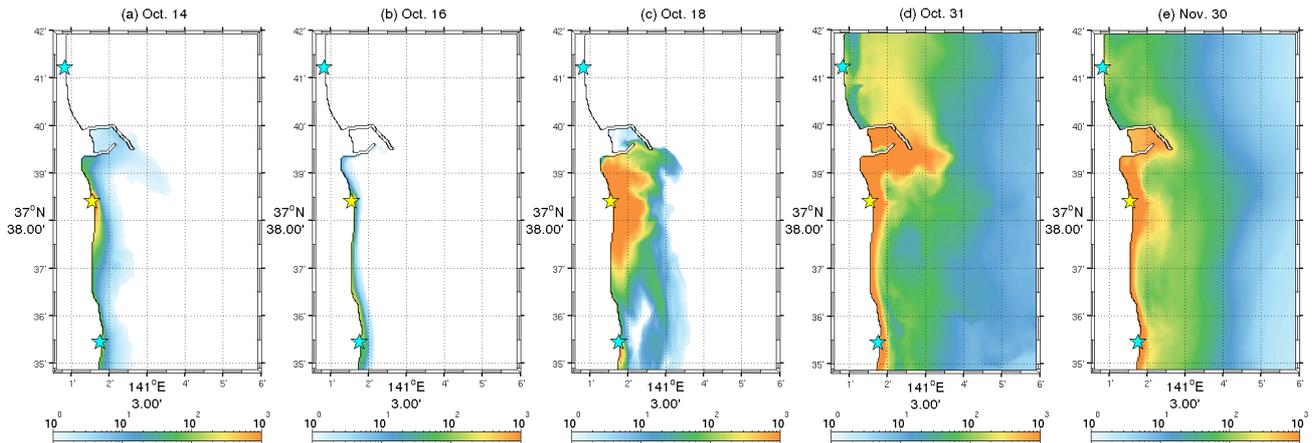
Figure 4: Temporal evolution of suspended ^{137}Cs in the marine bed sediments derived from Niida River (Bqm^{-2}). Daily averaged radioactivity in unit bed area is depicted for Oct. 14 (before Wipha), Oct. 16 (Wipha was closet to Niida River), Oct. 18 (two days after Wipha showing influences of heavy precipitation), Oct 31 (two weeks after Wipha), and Nov. 30 (six week after Wipha). The radioactivity is computed for all the three sediment size classes at 0:00 UTC on each day.

Table 3: Inventory of suspended ^{137}Cs originated from Niida River to the ocean. Cumulative radioactivity of suspended ^{137}Cs (unit: GBq) from Niida River (labeled by NR), and those accumulated in the six spatial segments (RM: river mouth at depths < 5 m, OM: offshore of the mouth at depths ranging between 5 and 10 m, NS: north shore area at depth < 10 m, SS: southern shore area at depth < 10 m, OS: offshore area, and OD: out of domain) are depicted. The area segmentation with their acronyms are presented in **Figure 1b**. Time integral was performed from Oct .1 to Oct. 14, Oct. 16, Oct. 18, and Nov. 30.

Date in 2013	NR	RM	OM	NS	SS	OS	OD
10/14	0.530	0.249	0.002	0.021	0.182	0.021	0.056
10/16	0.578	0.023	0.001	0.003	0.132	0.003	0.417
10/18	32.00	21.05	1.333	0.855	2.573	0.403	5.790
11/30	55.73	25.22	0.365	1.694	14.01	6.541	7.902

Concluding Summary

To summarize the present study, the suspended ^{137}Cs inventory was analyzed as listed in **Table 3**. Cumulative total radioactivity of suspended ^{137}Cs discharged out of Niida River (NR) was about 30 GBq until Oct. 18 (just after the typhoon passage), and about 56 GBq until Nov. 30. About 25 GBq (45.3 %) of this 56 GBq was deposited near the river mouth only within a radius of 1 km (RM). The offshore area of the mouth (OM) caught a quite limited amount of the riverine suspended ^{137}Cs; it increased to 1.3 GBq until Oct. 18, but then decreased to 0.37 GBq until Nov. 30, which is only ~1.5 % of that accumulated in the near-mouth region (RM). The decrease of the ^{137}Cs inventory in OM stands for erosive characteristic over there, with estimated spatial half-life of suspended ^{137}Cs of about three days. Alongshore transport of sediments and suspended ^{137}Cs occurred asymmetrically with an evident southward bias. The southern area of the Niida river mouth (SS) caught ^{137}Cs accumulation of ~14 GBq (25.1 % of the river-derived ^{137}Cs), whereas only 1.7 GBq was transported northward (NS). By contrast, the offshore and far-field transport were rather small; the offshore ^{137}Cs transport beyond the 10-m isobaths (OS) occurred ~6.5 GBq (11.7 %) and the far-field transport existing the model domain (OD) was 7.9 GBq (14.2 %), respectively. Therefore, the Niida river-derived ^{137}Cs mostly stayed in the southern nearshore area of the mouth.

It is worth noting that these model estimates are generally consistent with field measurements conducted near the Niida river mouth in the fall 2013. The quantitative model assessment of the river-originated radioactivity revealed that infrequent but non-trivial supplies of terrestrial ^{137}Cs have taken place occasionally to influence subsequent oceanic dispersal and resultant redistribution of deposited sediments and suspended ^{137}Cs in the ocean floor.

Acknowledgements

References

1   Tsumune, D., Tsubono, T., Aoyama, M., and Hirose, K., 2012: Distribution of oceanic ^{137}Cs from the Fukushima Dai-ichi Nuclear Power Plant simulated numerically by a regional ocean model. *J. Environ. Radioact*. **111**, 100–108. doi: 10.1016/j.jenvrad.2011.10.007

2   Tsumune, D., Tsubono, T., Aoyama, M., Uematsu, M., Misumi, K., Maeda, Y., Yoshida, Y., and Hayami, H., 2013: One-year, regional-scale simulation of ^{137}Cs radioactivity in the ocean following the Fukushima Dai-ichi Nuclear Power Plant accident, *Biogeosciences*, **10**, 5601–5617, doi:10.5194/bg-10-5601-2013

3   Kamidaira, Y., Uchiyama, Y., Kawamura, H., Kobayashi, T. and Furuno, A., 2018. Submesoscale mixing on initial dilution of the radionuclides released from the Fukushima Dai-ichi Nuclear Power Plant. *J. Geophys. Res. Oceans*, **123**, doi: 10.1002/2017JC013359

4   Misumi, K., Tsumune, D., Tsubono, T., Tateda, Y., Aoyama, M., Kobayashi, T., and Hirose, K., 2014: Factors controlling the spatiotemporal variation of (137) Cs in seabed sediment off the Fukushima coast: implications from numerical simulations. *J. Environ. Radioact*., **136**, 218–228, doi: 10.1016/j.jenvrad.2014.06.004

5   Shchepetkin, A.F., McWilliams, J.C., 2005. The regional ocean modeling system (ROMS): a split-explicit, free-surface, topography-following-coordinate oceanic model. *Ocean Model*. **9**, 347–404.

6   Miyazawa, Y., Zhang, R., Guo, X., Tamura, H., Ambe, D., Lee, J.-S., Okuno, A., Yoshinari, H., Setou, T. and Komatsu, K., 2009: Water mass variability in the western North Pacific detected in a 15-year eddy resolving ocean reanalysis. *J. Oceanogr*. **65**, 737-756.

7   Mason, E., Molemaker, M. J., Shchepetkin, A.F., Colas, F., McWilliams, J.C., Sangrà, P., 2010. Procedures for offline grid nesting in regional ocean models. *Ocean Model*. **35**, 1–15.

8   Uchiyama, Y., Kanki, R., Takano, A., Yamazaki, H. and Miyazawa, Y., 2017. Mesoscale reproducibility in regional ocean modeling with a 3-D stratification estimate based on Aviso-Argo data, *Atmosphere-Ocean*, **55**, 1–18, doi: 10.1080/07055900.2017.1399858

9   Uchiyama, Y., Suzue, Y. and Yamazaki, H., 2017. Eddy-driven nutrient transport and associated upper-ocean primary production along the Kuroshio, *J. Geophys. Res. Oceans*, **122**, 5,046–5,062, doi:10.1002/2017JC012847

10   Tada, H., Uchiyama, Y. and Masunaga, E., 2018. Impacts of two super typhoons on the Kuroshio and marginal seas on the Pacific coast of Japan, *Deep-Sea Res. Part I*, **132**, 80–93, doi: 10.1016/j.dsr.2017.12.007

11   Uchiyama, Y., Idica, E., McWilliams, J.C. and Stolzenbach, K.D., 2014: Wastewater effluent dispersal in Southern California Bays. *Cont. Shelf Res*., **76**, 36–52. doi:10.1016/j.csr.2014.01.002

12   Uchiyama, Y., Zhang, X., Suzue, Y., Kosako, T., Miyazawa, Y. and Nakayama, A., 2018. Residual effects of treated effluent diversion on a seaweed farm in a tidal strait using a multi-nested high-resolution 3-D circulation-dispersal model, *Mar. Pollut. Bull*., **130**, 40–54, doi: 10.1016/j.marpolbul.2018.03.007

13   Blaas, M., Dong, C., Marchesiello, P., McWilliams, J.C. and Stolzenbach, K.D., 2007: Sediment-transport modeling on Southern Californian shelves: A ROMS case study. *Cont. Shelf Res*., **27**, 832–853.

14   Soulsby, R. L., 1995: Bed shear-stresses due to combined waves and currents. In: *Advances in coastal morphodynamics*, eds, M. J. F. Stive, H. J. de Vriend, J. Fredsoe, L. Hamm, R. L. Soulsby, C. Teisson and J. C. Winterwerp, 4-20 to 4-23.

15   Booij, N., Ris, R.C. and Holthuijsen, L.H., 1999: A third-generation wave model for coastal regions 1. Model description and validation, *J. Geophys. Res*., **104**, C4, 7649 –7666.